Image Cover Sheet

CLASSIFICATION	SYSTEM NUMBER
UNCLASSIFIED	141641

TITLE

ELECTROCHEMICAL CHARACTERIZATION OF THE RESISTANCE OF Al-Li ALLOY SHEET TO SEAWATER CORROSION

AN: 94-03048

System Number:

Patron Number:

Requester:

Notes:

DSIS Use only:

Deliver to: BA

141691

9.

"Electrochemical Characterization of the Resistance of Al-Li Alloy Sheet to Seawater Corrosion"

P.R. Roberge, E. Halliop

Royal Military College, Kingston, Ont.

D. Lenard, and J.G.M. Moores

DREP, Victoria, B.C.

Electrochemical Characterization of the Resistance of Al-Li Alloy Sheet to Seawater Corrosion

P.R. Roberge and E. Halliop
Department of Chemistry and Chem. Eng., Royal Military College
Kingston, Ontario, K7K 5L0 (Canada)

D.R. Lenard and J.G.M. Moores
Materials Technology Section, Defence Research Establishment Pacific
FMO Victoria, B.C., V0S 1B0 (Canada)

Abstract

The electrochemical measurements obtained with the three orthogonal faces of commercial aluminum and aluminum-lithium sheet material were compared to the results obtained during the long term exposure of the same alloys to real sea water. The results obtained during this extensive study indicated that short term EIS measurements can help to predict the general and localized corrosion behavior of this material when exposed to sea water. A systematic analysis of 610 fifteen minute noise records with the stochastic pattern detector technique has demonstrated that the exponential decay model describes very well the potential fluctuations observed during these experiments, thereby confirming the random nature of the corrosion processes in progress. The parameters revealed during the noise analysis were additionally related to the features calculated from EIS measurements or observed after long term exposure of the same alloys in a flowing sea water tank.

Introduction

The development of a special group of aluminum alloys containing lithium as one of the primary alloying elements was described as the single largest R&D effort in the history of aluminum metallurgy[1]. The main advantage of alloying lithium to aluminum used in aerospace vehicles comes from the increased modulus of elasticity and strength, which are paralleled by a unique reduction of density of the alloys. The aluminum-lithium alloys can offer substantial (≈10%) weight savings over conventional aerospace aluminum alloys such as the 2000 and 7000 series. In addition, fatigue properties and corrosion resistance of aluminum alloys are said to improve by alloying them with lithium[2]. But past experience indicates that gains in mechanical properties are often taxed by a simultaneous increase of the susceptibility to catastrophic forms of corrosion. For example, the T6 temper of Aluminum Alloy (AA) 7075 was readily adopted by aircraft designers because of its high modulus and strength. It was subsequently discovered to be highly susceptible to stress corrosion and exfoliation in the marine environment[3], at great cost to aircraft operators. As a result of this history and because elemental lithium is extremely reactive, there has been considerable interest in the corrosion susceptibility of aluminum-lithium alloys.

A variety of accelerated corrosion tests[4-8] and standard electrochemical techniques[8-11] have been used to study the corrosion behavior of Al-Li. The resistance of aluminum alloys to stress corrosion cracking (SCC) has also been extensively studied in many laboratories around the world[4,10,12-18]. But the multitude of heat treatments which are possible, added to the variability of alloy compositions which have been studied, have resulted in an uncomfortable degree of uncertainty concerning the factors that control the initiation of localized corrosion on aluminum-lithium alloys. In order to acquire first hand experience with the behavior of these alloys in the marine environment, the Defence Research Establishment Pacific (DREP) subjected panels made from (AA)2090 and 8090 sheet, along with 2024 and 7075 sheet, to several tests involving exposure to sea water fog and full or part immersion in sea water[8]. The results of these tests were then compared with results obtained at the Royal Military College of Canada during the analysis of EIS and electrochemical noise measurements made with the same alloys exposed to synthetic sea water (3% NaCl).

Electrochemical Techniques

Electrochemical impedance spectroscopy (EIS)

Electrochemical Impedance Spectroscopy (EIS) has been successfully applied to the study of corrosion systems for almost twenty-five years. Since the early work published by Epelboin and co-workers[19] EIS has gained tremendous momentum and popularity in corrosion laboratories around the world. An important advantage of EIS over other laboratory techniques is the possibility of using very small amplitude signals without disturbing the properties being measured. EIS has also recently found its way into practical field applications[20-22] where its capability of working in difficult and changing hydrodynamic conditions can become a serious advantage once the complications of analyzing EIS results are overcome.

EIS has been shown to be a rapid, powerful and accurate method for measuring corrosion rates. But in order to access the charge transfer conductance, which is proportional to the corrosion rate at the monitored interface, the EIS results have to be understood with the help of a model of the interface. The simplest model representing such an interface must also include a capacitance which describes the capacitive charge acceptance of any metallic surface exposed to an electrolyte. The validation of this simple RC equivalent circuit model can be achieved by permuting the three data points selected to project the center of a circle in a Nyquist representation. The application of this principle to the study of various alloys exposed to aqueous environments has revealed that the non-adherence of the EIS measurements to a perfect RC model is a rich source of information[23] concerning the types of corrosion processes occurring on a metallic surface.

One omnipresent characteristic of the EIS spectra that must be addressed properly, in terms of its significance in corrosion studies, is the constant phase element (CPE) which is commonly introduced as an empirical factor in fitting procedures to describe the angle of tilt often visible in Nyquist plots. The empirical factor would then appear as an exponent β with a value between 0 and 1, which would be added to the imaginary component of an impedance frequency (ω) response $Z(\omega)$ (Eq. 1).

$$Z(\omega) = R_s + \frac{R_p}{1+(j\omega R_p C_{dl})^{\beta}} \quad (1)$$

A traditional explanation for the CPE has been surface dispersion effects[24-26] which, in the case of a corroding metal, have themselves been attributed to microscopic roughening of the surface[27-29] and more recently to typical defects produced by localized corrosion such as encountered when carbon steel[30-32] or aluminum alloys[33,34] are exposed to mildly corrosive environments.

Electrochemical noise (EN)

The most accepted technique to analyze noise data has been to transform time records in the frequency domain in order to obtain power spectra. Since noise signals can be produced by either deterministic or stochastic processes and often consist of a complex combination of these processes, a practical approach has been to correlate predominant frequencies and deconvolute unwanted signals in an iterative manner using well established mathematical functions[35].

The approach used in the present study for the analysis of voltage fluctuations has been extensively described elsewhere[36,37]. With this technique the voltage fluctuations are first transformed into individual voltage peaks as basic events. The rise time of the basic events (dV/dt) is then computed since this parameter is thought to be an important characteristic of the electrochemical systems being studied. During a second process of data transformation the probability distribution of the basic events is compared with a typical Poisson probability distribution of stochastic point processes. A measure of the goodness-of-fit is then evaluated by comparing the ideal exponential distribution to the experimental distributions observed and corresponding to individual λ_t calculated with Eq. 2 and subsequently averaged. The goodness-of-fit itself would be an expression of the difference between this average and the ideal value λ (Eq. 3).

$$\lambda_t = \frac{f(t)}{e^{-\lambda t}} \quad (2)$$

$$\text{Goodness-of fit}(\%) = \left(1 - \left|1 - \frac{\bar{\lambda}}{\lambda}\right|\right) \cdot 100\,\% \quad (3)$$

Experimental

Sea water exposure

The 76 x 76 mm panels used in the exposure tests were sheared from sheets made of Aluminum Alloys 2024-T3, 2090-T8, 7075-T6 and 8090-T851.The nominal composition of the alloys are shown in Table 1. Both surfaces of each panel were sanded with 120 grit silicon carbide abrasive paper and each panel was then fitted with two ceramic multiple-crevice washers (designed according to ASTM G78) that were held in place with a #12 stainless steel nut and bolt assembly that passed through a 6.3 mm central hole. Each bolt was fitted through plastic tubing to prevent contact with the aluminum panel. Each washer provided twelve separate sites for initiation of crevice

corrosion. Each panel was suspended by way of a plastic-coated wire that was passed through a 3 mm hole that had been drilled in one corner of the specimen.

SF850 Corrosive Fog Exposure System. The exposure was conducted according to ASTM B117 with the exception that natural sea water was used to generate the fog instead of the standard sodium chloride solution.

Partial and total immersion. The remaining specimens were suspended in sea water that was drawn from the Strait of Juan de Fuca and directed through a tank measuring 16 X 62 x 177 cm. The sea water flowed past any specimen immersed in it at a rate of 1 cm/sec and was then returned to the Strait 40 m from the intake. The water temperature in this location was within the range 7-11^{o}C. One set was suspended in a single row perpendicular to the direction of flow so that one half of the specimen was under water. A second set was suspended in a single row 1 m downstream from the first so that the entire specimen was immersed.

All specimens were removed after an exposure time of four months. After the specimens were dismantled, the aluminum panels were cleaned by immersion in concentrated nitric acid. They were then rinsed with distilled water and allowed to dry after a final rinse with ethanol. Sections were cut from the panels and set in epoxy according to standard metallographic techniques in an effort to determine the depth of corrosion that had been initiated at the edges of the specimens.

Electrochemical tests

The aluminum specimens were cut to appropriate sizes for mounting in epoxy according to metallographic techniques. The samples were mounted in a manner that would expose only one face of each of three orthogonal planes that were related to the rolling direction of the sheet (the rolled surface, the long transverse edge and the short transverse edge). Prior to mounting, provisions were made for electrical connection to the unexposed part of the samples, and the edges were coated with an aluminum-vinyl anti corrosive paint to prevent crevice corrosion between the epoxy mount and the aluminum electrodes. After mounting, the specimens were polished (using 240, 400 and finally 600 grit papers) and cleaned with acetone and dichloromethane.

For each experiment, a pair of identical aluminum specimens (same alloy and same exposed face) was immersed in a 2 l beaker containing a solution of 3% sodium chloride. Each cell was equipped with an air purge and a saturated calomel reference electrode brought into close proximity with one electrode by a Luggin probe. The mounted specimens were separated by 2.5 mm and kept in a stable parallel position with plastic holders. EIS measurements were performed with a commercial frequency response analyzer (Solartron Model 1255) at the corrosion potential. A potentiostat was not used in these measurements. The alternating current was applied between the two aluminum electrodes and kept at a value which would not cause more than 10 mV difference (peak to peak) across the cell.

The reference electrode served to measure the corrosion potential and its fluctuations which were monitored with a sensitive multimeter (HP model 3457) through a high pass filter (1 MΩ resistor in parallel to a 1 μF capacitor) which served to increase the sensitivity even further by nulling the DC voltage component. A custom-made

multiplexer controlled by a laboratory computer directed the inputs from each technique to a storage device. At the completion of these experiments, which lasted approximately two weeks, the specimens were removed and examined with both optical and scanning electron microscopy to observe any differences in corrosion morphologies.

Results and Discussion

The EIS data analysis technique mentioned earlier was used to calculate polarization resistance (R_p) values for each impedance plot gathered. These values were then converted into corrosion currents by multiplying them with a proportionality constant (B)[38] according to the Tafel extrapolation technique for measurement of corrosion kinetic parameters introduced by Stern[39] and Stern and Geary[40]. The corrosion current was itself converted into penetration rates using Faraday's law. The global equation is expressed in Eq. 4 where the corrosion rate is in mm/y when R_p is in $\Omega \cdot cm^2$. B is a proportionality constant for aluminum in chlorides (24 mV)[38], E.W. is the equivalent weight (9g) of aluminum (g/equiv.) and d its density ($2.7 g/cm^3$).

$$\text{Corrosion rate} = \frac{3.3 \cdot B \cdot E.W.}{R_p \cdot d} \qquad (4)$$

According to the EIS polarization resistance data, which are summarized in Table 2, the 8090 alloy showed roughly equal corrosion rates for all three faces. Except for the rolled face, the corrosion rate of the 8090 alloy was substantially lower than the corresponding faces of the 2024 alloy. With the assumption that the CPE, which is directly proportional to (1-β), increases in some manner with increased pitting, the EIS data indicated that the rolled surface of the 8090 had the lowest susceptibility to pitting, followed by the long transverse edge and the short transverse edge, which had the highest rate (Table 2). Examination of these surfaces with optical and scanning electron microscopy suggested that the correlation between the CPE and pitting rate involved the number of pits formed in any given area (pit density) rather than the pit depth. The low pitting rate suggested by EIS for the rolled surface was consistent with visual observation of the long term exposure panels. However, the approximate equivalence for all three faces was not. If the interpretation of EIS data is correct, the corrosion of the rolled surface must occur initially at this high rate, but then would fall to a much lower value over the longer term. The R_p values for the 2024-T3 alloy showed a pronounced difference in overall corrosion rate between its rolled surface and its edges, with the edges having consistently higher rates. After about 50 hours, a similar trend was observed for the CPE. These results are consistent with observations made on the long term exposure panels, which were characterized by a higher density of localized corrosion sites on the edges.

On the basis of the EIS data the conclusion would be reached that the edges of the 8090-T8 alloy had lower overall corrosion rates and were less prone to pitting than their 2024-T3 counterparts. The edges of the 8090 long term exposure panels had substantial areas where no visible corrosion had occurred. This could be consistent with the lower overall corrosion rates and lower pitting density suggested by EIS results in comparison with 2024. However, the depth of attack within each pit (Fig. 1) was as large or larger

than a corresponding pit on 2024. Thus the rate of corrosion within a pit was at least as severe for 8090 as for 2024.

As was the case for the 8090 alloy, the corrosion rate determined with EIS for the rolled surface of the 7075 was approximately equal to that measured for the edges. This was not consistent with the appearance of the long term panels, which suffered more metal loss along the edges than the rolled surface. The CPE values obtained for these experiments indicated that the rolled surface of the 7075 alloy had the lowest pitting density while the long and short edges had higher rates. The higher rates reached similar and essentially constant values after 200 hours. These results did correlate very well with the long term exposure tests, in which the edges did indeed suffer much worse localized attack.

According to the EIS results the rolled surface of the 2090 alloy had a consistently lower general corrosion rate than the same surface of the 7075. This did not appear to be consistent with the long term exposure tests, in which corrosion damage seemed to be more extensive on the surface of the 2090 alloy. On the other hand the EIS data suggested that the edges of the 2090 were only slightly more corrosion resistant than the 7075 edges. Once again this did not appear to be consistent with visual observation of the long term exposure panels. In this case the edges of the 2090 panels suffered noticeably less corrosion than their 7075 counterparts. The CPE data indicated that the pit density should be lower on the rolled surface of the 2090 than the 7075 and that the pit density should be much lower on the edges of the 2090 than the 7075. These results are completely consistent with the appearance of the long term exposure panels.

In an effort to correlate the parameters calculated by the exponential decay model, 610 records of fifteen-minute data gathered during the laboratory testing of the aluminum sheet material were compared to the results obtained on the same specimens with EIS or during the long term exposure to sea water. While the agreement between the noise patterns and the model seemed to be excellent (average Goodness-of-fit = 97.2% (Eq. 3)), no simple correlation could be found between any of the calculated parameters and the general corrosion rates evaluated with EIS. Such a conclusion would confirm what others[41,42] had found previously, i.e. the degree of potential fluctuations at the corrosion potential is a relatively insensitive indication of general corrosion rates.

Fig. 2 illustrates the global behavior of the average rising time measured on all three faces of 8090-T8 sheet material for each of the noise data record gathered during the experiments, when plotted as a function of corrosion potential. These two parameters were chosen for this global representation of the results because they were thought to reflect the fundamental behavior of the equilibria being established during the continuous corrosion of aluminum specimens. It was observed that the four alloys tested behave quite differently during these two week experiments.

The predominance of the high rise time values in the anodic fraction of these plots seems to be related to the good performance of an alloy and is probably associated with the control of the corrosion processes by passivation (anodic potentials). An electrical analogy would be an open circuit situation with fast unbuffered switching of the potential. The relative fraction of slow transients was quantified (everything that is not in the left uppermost corner of Fig. 2) and these fractions were compared (Fig. 3) to the average corrosion rates measured with EIS (Table 2).

While the correlation coefficient between the two variables presented in Fig. 3 seems to be excellent (r = 0.99) the relation itself has to be interpreted with some caution since the time of exposure, which is not represented in these comparisons, would have a strong influence on the absolute values estimated for the predominance of fast transients which were always more prevalent during the first few days of each experiment and tapered off as exposure time progressed.

Conclusion

The long term exposure tests indicated that the rolled surfaces of the 8090-T851 sheet were more resistant to corrosion than the conventional 2024-T3 sheet. Except for some pits which developed at an air/water interface, these surfaces suffered only minor corrosion. The same tests indicated that the rolled surfaces of the 2090-T8 sheet suffered as much or even more corrosion damage than their counterparts on the 7075-T6 sheet. Some fairly deep pits occurred on the rolled surfaces of the 2090, even during the exposure to sea water fog.

The results obtained during the electrochemical testing of various faces of aluminum sheet material indicated that short term EIS measurements can help to predict the general and localized corrosion behavior of this material when exposed to sea water. In fact the prediction of the localized corrosion behavior with the CPE calculated from the EIS data seemed to agree more closely to the long term tests results than the general corrosion estimation. A systematic analysis of 610 fifteen minute noise records with the stochastic pattern detector technique has also demonstrated that the exponential decay model describes almost perfectly the potential fluctuations observed during these experiments, thereby confirming the random nature of the corrosion processes in progress. The parameters revealed during the noise analysis could additionally be globally related to the features calculated from EIS measurements.

References

1. W. E. Quist and G. H. Narayanan, "Aluminum-Lithium Alloys," in A. K. Vasudevan and R. D. Doherty, Eds., Treatise on Materials Science and Technology, Academic Press, New York, 31 (1989), p. 219.
2. D.B. Williams and P.R. Howell, "The Microsstructure of Aluminum-Lithium Base Alloys," in A. K. Vasudevan and R. D. Doherty, Eds., Treatise on Materials Science and Technology, Academic Press, New York, 31 (1989), p. 364.
3. S.J. Ketcham and J.J. de Luccia, Aircraft Corrosion, AGARD Conference Proceedings No. 315 (1981).
4. C.J.E. Smith et al., "New Light Alloys," AGARD Conference Proceedings No. 444, Mierlo, Netherlands, 3-5 October 1988, p. 7-1.
5. T.S. Srivatsan, "Microstructure Compatibility of an Al-Li-Cu-Mg-Zr Alloy Exposed to Corrosive Environmenst," Report AD-A215 540, Naval Surface Weapons Center, White Oak, MD, USA (1987).
6. J. Kozol et al., "In-Service Evaluation of 2090 Aluminum-Lithium Alloy on F/A-18 Aircraft," Report AD-A248 472, Naval Air Systems Command, Washington, DC, USA (1991).
7. J.P. Moran et al., Corrosion, 43 6 (1987): p. 374.

8. D.R. Lenard, J.G. Moores. P.R. Roberge and E. Halliop, Marine Corrosion of Aluminum-Lithium Aloy Sheet, TTCP-P-TP1 Report, Defence Research Establishment Pacific, Victoria, Canada (1991).
9. R.G. Buchheit Jr., J.P. Moran and G.E. Stoner, Corrosion, 46 8 (1990): p. 610.
10. M. Habashi, Corrosion Science, in press.
11. A. Roth and H. Kaesche, "Electrochemical Investigation of Technical Aluminum-Lithium Alloys," Proceedings of Aluminum-Lithium Alloys, Williamsburg, VA, USA (1989), p. 1196.
12. R.C. Dorward, Materials Science and Engineering, 84 (1986): p. 89.
13. R.C. Dorward and K.R. Hasse, Corrosion, 44 12 (1988): p. 932.
14. B. Bavarian et al., "Localized Corrosion of 2090 and 2091 Al-Li Alloys," Proceedings of Aluminum-Lithium Alloys, Williamsburg, VA, USA (1989), p. 1227.
15. A. Buis and J. Schijve, Corrosion, 48 11 (1992): p. 898.
16. E.S.C. Chin et al., "Evaluation of 2090-T8E48 Aluminum-Lithium Plates," Report AD-A217 262, U.S. Army Materials Technology Laboratory, Watertown, MA, USA (1989).
17. C. Kumai et al., Corrosion, 45 4 (1989): p. 294.
18. T. Sheppard and N.C. Parson, Materials Science and Technology, 3 (May 1987): p. 345.
19. I. Epelboin, M. Keddam and H. Takenouti, Journal of Applied Electrochemistry, 2 (1972): p. 71.
20. V.S. Sastri and P.R. Roberge, "Monitoring Corrosion in Sour Media," Materials Performance: Sulphur and Energy, P.R. Roberge et al., Eds., The Canadian Institute of Mining, Metallurgy and Petroleum, Montreal, 1992, pp. 57-69.
21. P.R. Roberge and V.S. Sastri, CORROSION 93, Paper No. 396, (National Association of Corrosion Engineers; Houston, TX, 1992).
22. P.R. Roberge and V.S. Sastri, Corrosion Science, in press.
23. P.R. Roberge, "Analyzing Simulated Electrochemical Impedance Spectroscopy Results by the Systematic Permutation of Data Points," Electrochemical Impedance Analysis and Interpretation, D.C. Silverman and J.R. Scully, Eds., ASTM STP 1188, American Society for Testing of Materials, in press.
24. K.S. Cole and R.H. Cole, Journal of Chemical Physics, 9 4 (1941): p. 341.
25. B.W. Davidson and R.H. Cole, J. Chemical Physics, 19 12 (1951): p. 1484.
26. A.K Jonscher, Dielectric Relaxation in Solids, (Chelsea Dielectrics Press, London, U.K., 1983).
27. R. De Levie, Electrochimica Acta,, 10 (1965): p. 113.
28. P.H. Bottelbergs and G.H.J. Broers, Journal of Electroanalytical Chemistry, 72 (1976): p. 257.
29. J.B. Bates, J.C. Wang and Y.T. Chu, Solid State Ionics, 18&19 (1986): p. 1045.
30. P.R. Roberge, E Halliop, M. Asplund and V.S. Sastri, Journal of Applied Electrochemistry, 20 (1990): p. 1004.
31. P.R. Roberge, "Analyzing Electrochemical Impedance Corrosion Measurements by the Systematic Permutation of Data Points," Computer Modeling in Corrosion,

R.S. Munn, Ed., ASTM STP 1154, (American Society for Testing of Materials 1992), p. 197.
32. P.R. Roberge, E. Halliop and V.S. Sastri, Corrosion, 48 6 (1992): p. 447.
33. P.R. Roberge, E. Halliop, D. Lenard and J. Moores, Corrosion Science, in press.
34. P.R. Roberge, E. Halliop, D. Lenard and J.G. Moores, "Marine Corrosion Behavior of Al-Li Alloy Sheet," 3rd. Int. SAMPE Metals and Metals Processing Conf., Toronto, October 20-22, 1992, p. M51.
35. J.S. Bendat and A.G. Piersol, Random Data: Analysis and Measurement Procedures, 2nd Ed, (John Wiley & Sons, New York, 1986).
36. P.R. Roberge, M. Farahani and K. Tomanstchger, Journal of Power Sources, 41 3 (1993): p. 321.
37. P.R. Roberge, Journal of Applied Electrochemistry, in press.
38. R. Grauer, P.J. Moreland and G. Pini, A literature review of polarisation resistance constant (B) values for the measurement of corrosion rate, (National Association of Corrosion Engineers, Houston, TX, 1982).
39. M. Stern, Corrosion, 14 (1958): p. 440.
40. M. Stern and A.L. Geary, Journal of the Electrochemical Society, 104 (1957): p. 56.
41. Lumsden, M.W. Kendig and S. Jeanjaquet, Corrosion92, Paper No. 224, (National Association of Corrrosion Engineers, Houston, TX, 1992).
42. Eden, K. Hladky and D.G. John, Corrosion86, Paper No. 274, (National Association of Corrosion Engineers, Houston, TX, 1986).

Table 1 Nominal composition of alloys tested (wt %).

Alloy	Li	Cu	Mg	Si	Fe	Mn	Zn	Zr
2024	-	3.8-4.9	1.2-1.8	0.5	0.5	0.3-0.9	0.25	-
2090	1.9-2.6	2.4-3.0	0.25	0.1	0.12	0.05	0.1	0.08-0.15
7075	-	1.2-2.0	2.1-2.9	0.4	0.5	0.3	5.1-6.1	-
8090[a]	2.35	1.23	0.67	0.02	0.03	0.001	0.02	0.11

Note a: Actual heat analysis for the specimens supplied by ALCAN

Table 2 Analyzed EIS results obtained with aluminum alloys.

Alloy	Thickness (mm)	Face	Corrosion Rate (mm/y)	β -
2024-T3	1.0	Rolled	0.05	0.81
		Long	0.16	0.77
		Short	0.22	0.75
2090-T3	1.2	Rolled	0.06	0.89
		Long	0.08	0.82
		Short	0.09	0.79
7075-T6	1.0	Rolled	0.14	0.87
		Long	0.11	0.63
		Short	0.12	0.68
8090-T8	1.5	Rolled	0.05	0.93
		Long	0.04	0.87
		Short	0.03	0.81

Table 3 Results of sea water exposure.

Alloy	Fog		Immersion		
			Partial		Total
	general	crevice	general	interface	
2024-T3	pitting	6 sites	severe pitting	severe pitting	severe pitting
2090-T3	few deep pits	none	"poultice"	severe	scattered pits
7075-T6	pitting	1 site	"poultice"	severe	scattered pits
8090-T8	minor	1 site	minor	few deep pits[a]	minor

[a] Figures 1a and 1b.

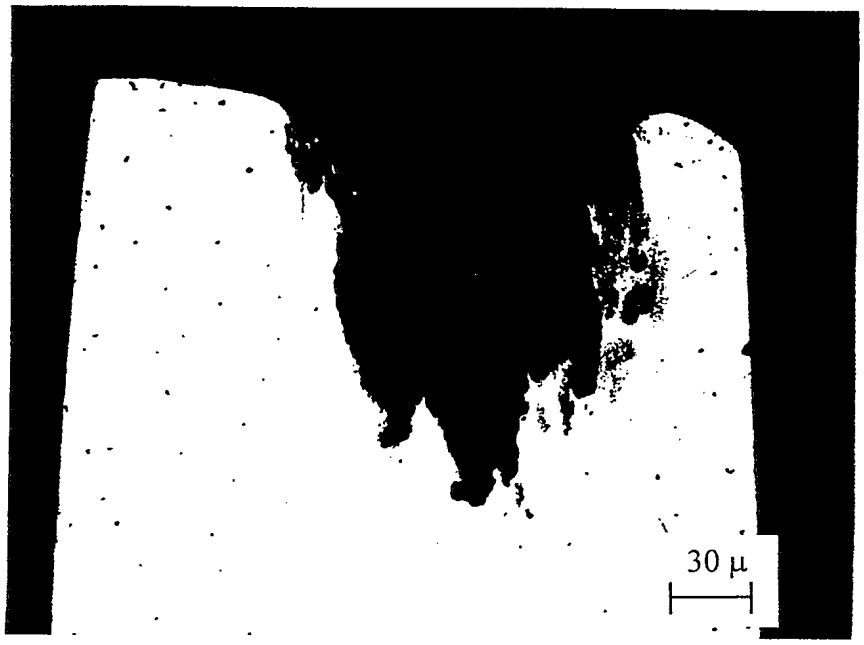

a)

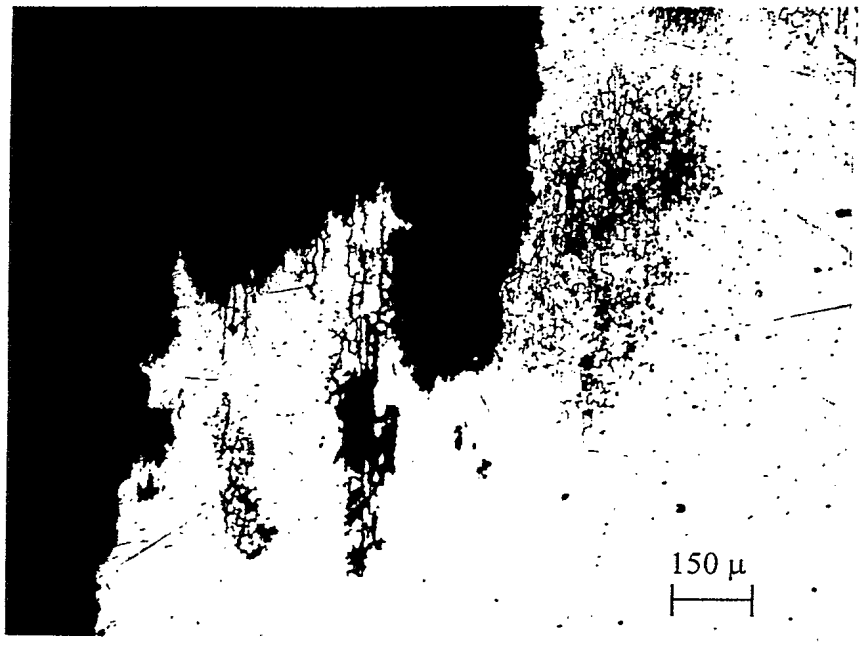

b)

Fig. 1 Metallograph of a section through an edge of the 8090 panel immersed in sea water during four months; a) at 64x and b) at 320x to illustrate the intergranular nature of the corrosion attack.

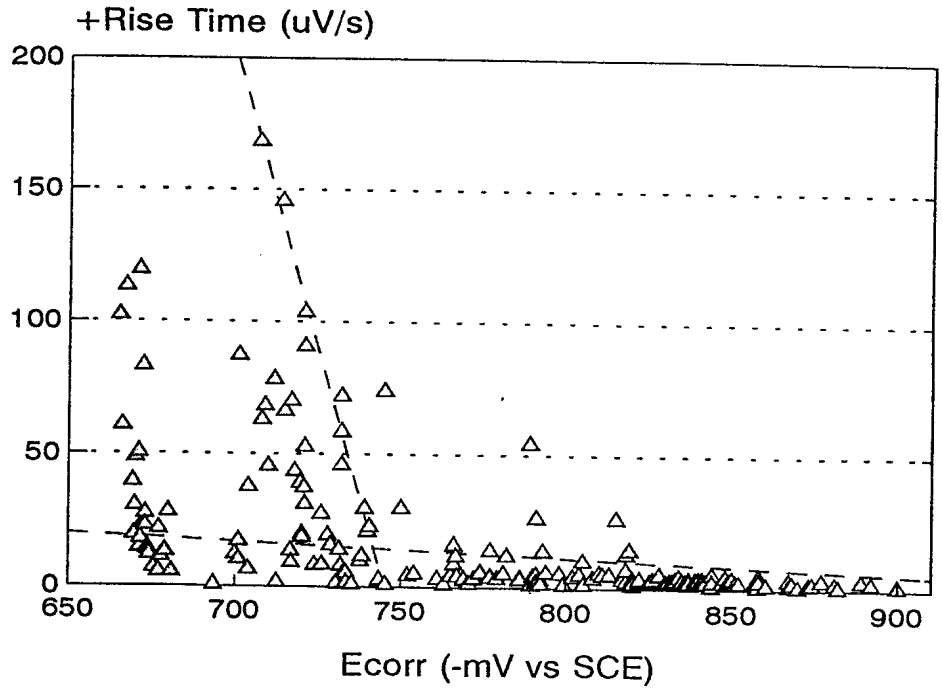

Fig. 2 Positive rise time calculated for each of 128 noise records gathered during the laboratory testing of 2090-T3 sheet material as a function of the corrosion potential.

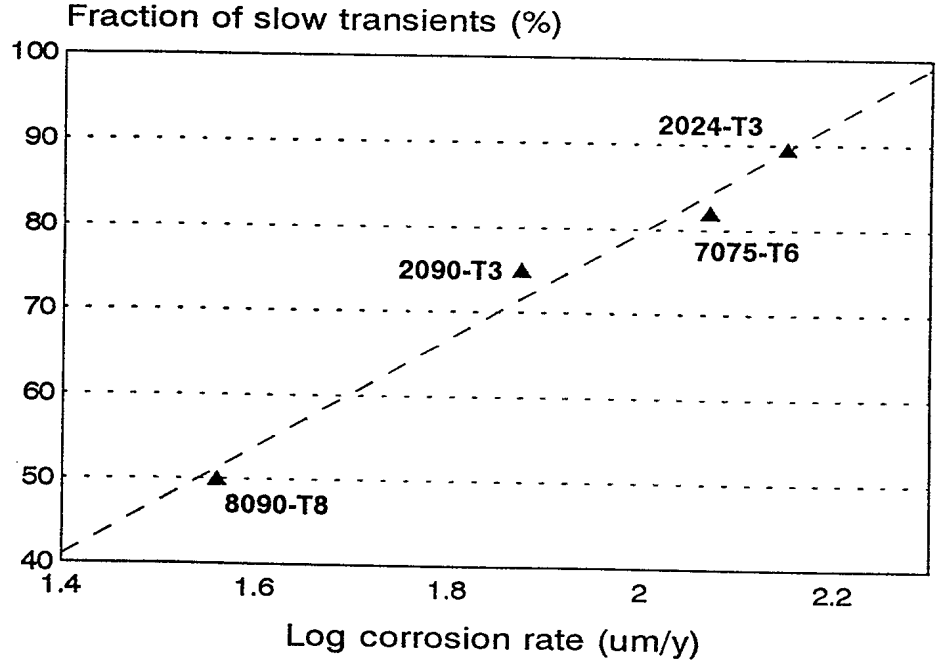

Fig. 3 Fraction of slow potential transients as a function of average corrosion rates.